



# CT Image Denoising using Discrete Wavelet Transform

Swapna Katta<sup>1,\*</sup> and Deepak Garg<sup>1</sup>

<sup>1</sup>School of Computer Science and Artificial Intelligence, SR University, Warangal, India

## Abstract

Low Dose Computed Tomography (LDCT) scan is modern medical imaging diagnostic technique that provides a detailed projection of internal human body tissue level structures. Even though the LDCT image quality is compromised by Gaussian-noise, which can be generated during image acquisition, this compromises the accurate diagnostic precision. The effective denoising is required to improve image quality in LDCT images. This study demonstrates that the Discrete Wavelet Transform(DWT) method shows better results, both quantitatively and visually, under varying noise intensities ( $\sigma = 10, 20, 30$ , and  $40$ ). The DWT method decomposes the image to multiresolution subbands (approximation, and detail) to provide localized analysis of structural patterns. The thresholding method is applied to the detail (noisy) coefficients and then reconstructs the refined image from these denoised coefficients. The DWT method achieved superior noise suppression while preserving edge information. The quantitative analysis among various methods, including PCA, MSVD, DCT, and DWT, consistently shows superior results, achieving a higher PSNR of 33.85 dB, SNR of 28.50 dB, and SSIM of 0.7194 at a noise level  $\sigma = 10$ . Among all denoising methods, the

DWT is a powerful and consistent method in image processing to enhance image quality in LDCT images.

**Keywords:** CT image, denoising Gaussian noise, DWT, Transform domain.

## 1 Introduction

Image denoising is a crucial preprocessing step in medical imaging, especially in CT scans, which influences the image accuracy in necessary tasks such as segmentation and relevant feature extraction. Since the development of CT scan in the years 1970s, it has played a major role in medical imaging diagnosis [1]. However, subsequent CT scans exposure patients to higher radiation doses, raising susceptibility to radiation-related health disorders such as cancer and hereditary genetic anomalies. To resolve these, safety concerns such as Low dose CT (LDCT) imaging have been developed to reduce X-radiation tube voltage and scan time. However, this results in noise in images and streak artifacts, degrading diagnostic image interpretation. LDCT images are often corrupted with Gaussian noise or Poisson noise during image acquisition process, resulting blurriness, thereby reducing diagnostic accuracy. Gaussian noise is extensively investigated and considered noise model in medical CT imaging. It proficiently illustrates electronic sensor-based noise, thermal differences, and reconstruction errors. Gaussian noise follows



Submitted: 31 July 2025

Accepted: 31 August 2025

Published: 22 September 2025

Vol. 1, No. 2, 2025.

10.62762/BISH.2025.874472

\*Corresponding author:

✉ Swapna Katta

[swapnakondam1@gmail.com](mailto:swapnakondam1@gmail.com)

## Citation

Katta, S., & Garg, D. (2025). CT Image Denoising using Discrete Wavelet Transform. *Biomedical Informatics and Smart Healthcare*, 1(2), 44–51.



© 2025 by the Authors. Published by Institute of Central Computation and Knowledge. This is an open access article under the CC BY license (<https://creativecommons.org/licenses/by/4.0/>).

a mathematical Gaussian distribution, characterized by its mean and standard deviation, making it suitable for algorithm design and facilitating a systematic comparison of various denoising methods. Furthermore, many other denoising models, such as Wavelet Shrinkage, CNN frameworks, and deep learning models, are upgraded and validated using Gaussian estimations, confirming reliability and replicability for controlled evaluations.

Therefore, it is necessary to develop denoising algorithms to mitigate Additive White Gaussian noise and improve imaging quality. Recent research mainly focuses on enhancing LDCT imaging quality using various denoising techniques [2]. LDCT imaging has emerged as a preferred technique for lung cancer-screening, cardiovascular examination, extended monitoring because it reduces radiation dose compared to other traditional techniques. An effective clinical solution for precise representation of Organs-at-risk (OAR) is necessary to provide safe image guided radiation therapy (IGR) for head and neck cancer, however, manual contouring is computationally intensive and tends to inconsistency. Recent studies have shown that deep learning-based auto segmentation considerably minimizes contouring time while elevating inter-observer reliability and efficacy of treatment planning. A Novel 3D lightweight architecture was trained and validated using multi center datasets to enhance clinical workflow and improve diagnostic outcomes. Effective denoising provides lesion conspicuity, thereby improving consistency in radiomic imaging biomarkers and reducing false positives in clinical screening programs [3, 4].

Image denoising techniques can be categorized into conventional denoising methods and nonconventional denoising methods [5]. Conventional denoising methods such as Spatial domain, Transform domain and the Hybrid methods. Spatial filters are applied to image raw pixel values, including Mean, median, Bilateral, Gaussian filters, which smooth the image by applying average neighborhood pixels but may often blur fine image details. The Transform domain methods transform the CT image into a different domain (multiresolution, frequency) in which the noise and signal can be separated in a better way. Initially, CT image is split into approximation (smooth or coarse) and detail coefficients (high frequency or noisy) to suppress the noise. Then, hard or soft thresholding is applied on detail coefficients to mitigate noise effectively.

Thresholding is the main denoising phase to remove small noisy coefficients while preserving significant details. Finally, inverse wavelet transform is used to reconstruct the denoised image. Transform domain methods such as Discrete Wavelet transform [6], PCA [7], Discrete Cosine transform [8], Curvelet transform [9], and Multiresolution singular value decomposition (MSVD) [10]. The hybrid methods [11] combine the spatial and transform-domain denoising methods to leverage complementary strengths, such as Total variation, and BM3D, and other denoising methods to provide locally smooth images and structural preservation. These transforms effectively suppress noise while preserving fine details in LDCT images.

Deep learning-based denoising methods train the neural-network to automatically learn from the noisy CT image to its equivalent clean image by observing a vast number of paired datasets [12, 13]. These methods include CNNs, GANs, and ResNets etc. CNNs are used in extracting spatial image features to reconstruct the clean images. A GAN network, including a generator network to generate denoised CT images, and a discriminator network to analyze authenticity. The system is trained in an adversarial way, has the ability to produce realistic output images by reducing differences between generated CT and true CT images. ResNet denoises the CT images using skip connections for easier training of the data. Transformer-based denoising models [14, 15] utilize self-attention mechanisms to extract long range associations and global contextual data. The transformer models such as ViT and Swin transformer are used to capture global and local dependencies in CT image.

## 2 Methodology

### 2.1 DWT Algorithm

The overall workflow of the proposed DWT-based denoising approach is illustrated in Figure 1. Let  $X_{i,j}$  denote the noisy input image.

#### Step1: Wavelet decomposition

Decompose the Noisy CT image  $X_{i,j}$  using two dimensional 2D Wavelet transform (DWT) up to the level  $L'$

$$\left\{ \mathbf{fA}_L, \{ \mathbf{fH}_1, \mathbf{fV}_1, \mathbf{fD}_1 \}_{l=1}^{L'} \right\} = \text{DWT} \left( \mathbf{X}_{i,j}, \psi, L' \right) \quad (1)$$

where  $\mathbf{fA}_L$  is the Approximation coefficients of level  $L$ ,  $\{ \mathbf{fH}_1, \mathbf{fV}_1, \mathbf{fD}_1 \}$  are the Horizontal, Vertical, and Diagonal detail-coefficients at level  $L'$ .

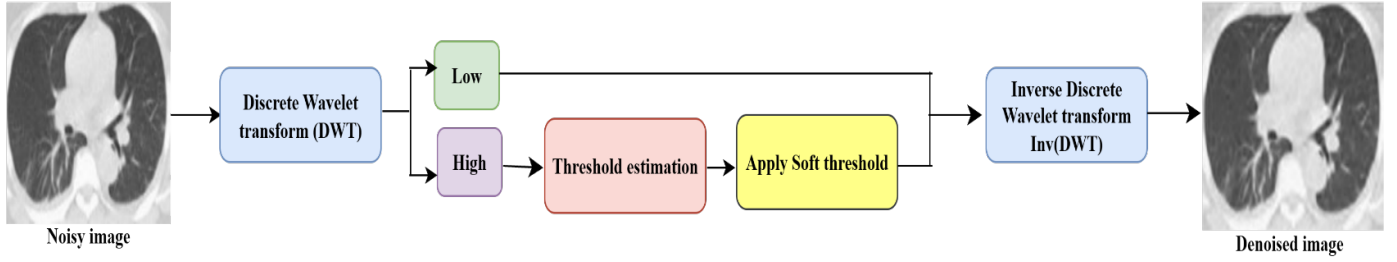


Figure 1. Flowchart of the DWT methodology.

**Step 2:** Estimate the noise level from High frequency subbands

Utilize the fine level diagonal coefficients  $\mathbf{fD}_L$  to estimate the standard deviation of noise in LDCT image

$$\sigma_{\text{esti}} = \frac{\text{median}(|\mathbf{fD}_L|)}{0.6745} \quad (2)$$

**Step 3:** Calculate Adaptive soft-threshold

Determine the soft thresholding value using the evaluated noise level

$$T_n = K \cdot \sigma_{\text{esti}} \quad (3)$$

where the constant K controls how significantly the wavelet-coefficients are shrunk.

A standard universal threshold method where:

$$K = \sqrt{2 \ln(N)} \quad (4)$$

N- Number of pixels in the CT image

K- Thresholding constant

K is adaptively adjusted for each subband or noise intensity level. A higher K value suppresses more noise but often leads to over-smoothing of the images, while smaller K values preserve image features but may retain residual noise. In order to generalizability, K is optimized using Stein's Unbiased Risk Estimate (SURE) or a cross-validation method, making it robust over various noise types and CT image datasets.

**Step 4:** Utilize soft thresholding to the detail coefficients

For each level ( $l = 1$ ) to L, apply the soft thresholding for all detail-subbands

$$\begin{aligned} \mathbf{fH}'_1 &= \text{soft}(\mathbf{fH}_1, T_n), \\ \mathbf{fV}'_1 &= \text{soft}(\mathbf{fV}_1, T_n), \\ \mathbf{fD}'_1 &= \text{soft}(\mathbf{fD}_1, T_n) \end{aligned} \quad (5)$$

where Soft thresholding can be computed as:

$$\text{Soft}(X_{i,j}, T_n) = \begin{cases} \text{sign}(X_{i,j}) \cdot (|X_{i,j}| - T_n), & \text{if } |X_{i,j}| > T_n \\ 0, & \text{otherwise} \end{cases} \quad (6)$$

**Step 5:** Wavelet reconstruction

Reconstruct the denoised CT image using inverse DWT transform

$$\widetilde{Y}_{i,j} = \text{DWT}_{\text{Inv}} \left( \left\{ \mathbf{fA}_L, \{ \mathbf{fH}_1, \mathbf{fV}_1, \mathbf{fD}_1 \}_{l=1}^{L'} \right\} \right) \quad (7)$$

where  $Y_{i,j}$  is the reconstructed denoised CT image,  $\text{DWT}_{\text{Inv}}$  is the inverse Discrete Wavelet Transform.

## 2.2 Explanation

Initially, the denoised process starts with an Additive Gaussian noisy image.

$$X_{i,j} = Y_{i,j} + \epsilon \quad (8)$$

where  $Y_{i,j}$  is the clean image, and  $\epsilon = N(0, \sigma^2)$  is the Additive Gaussian noise, and N represents the normal distribution, with a mean value of 0, and  $\sigma^2$  represents noise variance.

In the DWT transform, the noisy CT image  $X_{i,j}$  is decomposed into a low frequency (approximation- $\mathbf{fA}_L$ ), and high frequency (detail- $\mathbf{fH}_1, \mathbf{fV}_1, \mathbf{fD}_1$ ) coefficients. Noise primarily exists in the detail coefficients. After that, estimate the noise variance using median absolute deviation method. To mitigate the estimated noise, the threshold method  $T_n$  is applied in each detail coefficients ( $\{\mathbf{fH}_1, \mathbf{fV}_1, \mathbf{fD}_1\}$ , Horizontal, Vertical, and Diagonal) to preserve fine details in LDCT images. After the thresholding process, the denoised coefficients are transferred to the inverse DWT transform to reconstruct the denoised image  $\widetilde{Y}_{i,j}$ , specifically in the spatial domain. The DWT multiresolution approach provides localized noise reduction and fine structural preservation. The quality of the denoised CT image is assessed using PSNR, SNR, and SSIM metrics.

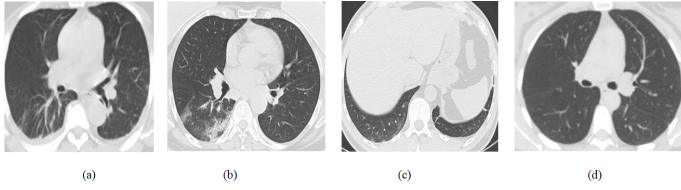


Figure 2. CT image dataset.

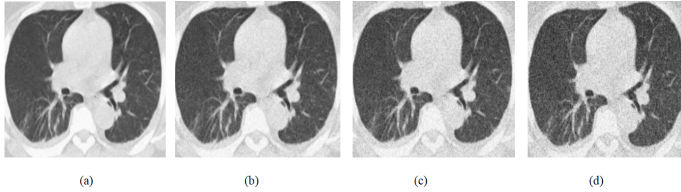


Figure 3. Noisy CT1 image from dataset with Additive Gaussian noise variance ( $\sigma$ )= (a) 10, (b) 20, (c) 30, (d) 40.

This method is especially effective in clinical images due to its capability to improve overall diagnostic imaging quality and clarity. DWT-based denoising is easily interpretable and computationally efficient for practical diagnostic applications.

### 3 Experiments

The clean CT images are taken from SARS-CoV-2 CT dataset [16] and are shown in Figure 2. The SARS-CoV2 dataset is used in this study to represent low dose CT scenarios. This publicly available dataset consists of a total of 2482 CT scan images, comprising 1252 COVID-19 positive cases and 1,230 are noninfected cases, collected from hospitals in Sao, Paulo, and Brazil. This dataset is mainly used to support research studies on AI-based techniques for COVID-19 detection in LDCT images. Figure 3 indicates the Gaussian noisy images of CT image1 with noise variance ( $\sigma = 10, 20, 30, 40$ ) to analyze the denoising capability of the DWT algorithm.

#### 3.1 Quantitative analysis

The Quantitative evaluation metrics [17] are represented as follows:

##### Peak signal to noise ratio (PSNR) :

PSNR is used to compare the peak possible power of a clean image's signal with the distorting power of the noise.

$$\text{PSNR}(Y_a, \hat{Y}_a) = 20 \cdot \log_{10} \left( \frac{\text{MAX}_i}{\text{RMSE}(Y_a, \hat{Y}_a)} \right) \quad (9)$$

##### Root mean squared error (RMSE):

RMSE is used to measure the absolute difference between original clean and the denoised CT image. Lower MSE represents a better denoised image, i.e, lower discrepancies between reference and denoised images.

$$\text{RMSE} = \sqrt{\sum_{i=1}^N (Y_a(i, j) - \hat{Y}_a(i, j))^2} \quad (10)$$

where  $\text{MAX}_i$  represents maximum pixel intensity values of 255 for 8-bit images.  $Y_a$  represents clean image.  $\hat{Y}_a$  represents denoised image. N Total number of pixel values in the image.

##### Signal to Noise ratio (SNR):

SNR is a quantitative measure to assess the image quality using the power of the clean image and the noise generated after denoising process.

$$\text{SNR}(Y_a, \hat{Y}_a) = 20 \cdot \log_{10} \left( \frac{\|Y_a\|_2}{\|Y_a(i, j) - \hat{Y}_a(i, j)\|_2} \right) \quad (11)$$

where  $\|Y_a\|_2$  is the L2 norm of the clean image (signal-power amplitude),  $\|Y_a(i, j) - \hat{Y}_a(i, j)\|_2$  is the noise amplitude.

##### Structural Similarity Index Measure (SSIM) :

It defines how well the reconstructed or denoised CT image preserves visual features of the ground-truth or clean CT image. The possible range of SSIM value is between 0 and 1. A high SSIM value of 1 indicates perceptually better quality between a clean and denoised image.

$$\text{SSIM}(Y_a, \hat{Y}_a) = \frac{(2\mu_Y\mu_{\hat{Y}} + C_1)(2\sigma_Y\sigma_{\hat{Y}} + C_2)}{(\mu_Y^2 + \mu_{\hat{Y}}^2 + C_1)(\sigma_Y^2 + \sigma_{\hat{Y}}^2 + C_2)} \quad (12)$$

where  $(Y_a, \hat{Y}_a)$  represents ground-truth and predicted denoised CT image.  $\mu_Y\mu_{\hat{Y}}$  represents mean values of the ground-truth and predicted denoised CT images.  $\sigma_Y\sigma_{\hat{Y}}$  represents variances of ground truth and predicted denoised ones.  $C_1, C_2$  are small constant values for stabilizing the division operation.

#### 3.2 Zooming Analysis

#### 4 Discussion

Table 1 shows a comparative analysis of four CT imaging denoising techniques, such as PCA [7], MSVD [10], and DCT [8] and DWT [6] at Gaussian noise intensities 10, 20, 30, and 40. The denoising performance is assessed using PSNR metric, among



**Table 1.** PSNR values of different denoising methods at Noise variance ( $\sigma = 10, 20, 30, 40$ ).

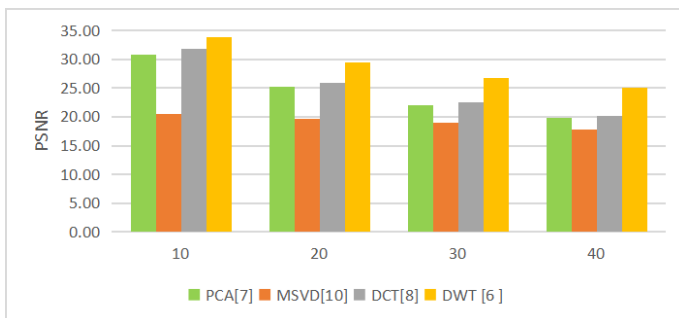
Denoising technique	Noise Variance			
	10	20	30	40
PCA[7]	30.84	25.19	22.02	19.85
MSVD[10]	20.49	19.58	18.99	17.85
DCT[8]	31.82	25.93	22.57	20.19
DWT[6]	33.85	29.40	26.82	24.99

**Table 2.** SNR values of different denoising methods at Noise variance ( $\sigma = 10, 20, 30, 40$ ).

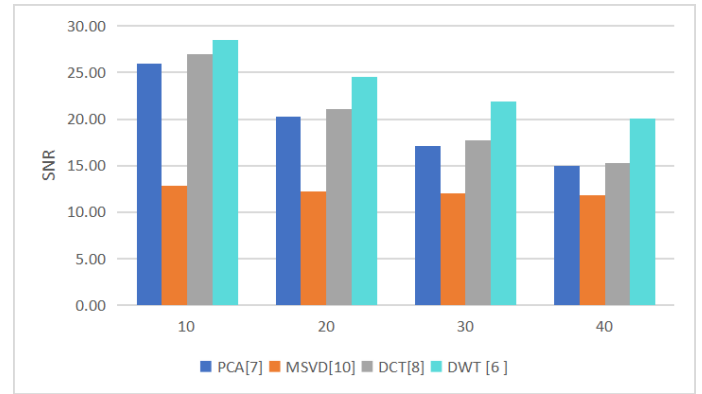
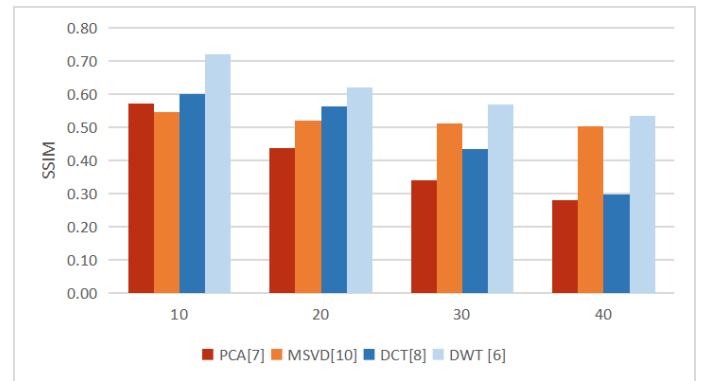
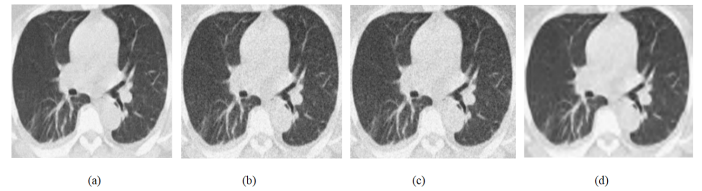
Denoising technique	Noise Variance			
	10	20	30	40
PCA[7]	25.95	20.30	17.13	14.96
MSVD[10]	12.89	12.20	11.99	11.87
DCT[8]	26.93	21.04	17.68	15.30
DWT[6]	28.50	24.54	21.90	20.10

**Table 3.** SSIM values of different denoising methods at Noise variance ( $\sigma = 10, 20, 30, 40$ ).

Denoising technique	Noise Variance			
	10	20	30	40
PCA[7]	0.57	0.44	0.34	0.28
MSVD[10]	0.56	0.52	0.51	0.50
DCT[8]	0.60	0.57	0.45	0.30
DWT[6]	0.72	0.62	0.57	0.53

**Figure 4.** Graphical representation of PSNR values of various denoising methods at Noise variance ( $\sigma = 10, 20, 30$  and  $40$ ).

all standard denoising methods, DWT obtains highest PSNR value at all noise levels ( $\sigma = 10$  (PSNR 33.85 dB),  $\sigma = 20$  (29.40 dB),  $\sigma = 30$  (26.82 dB), and  $\sigma = 40$  (PSNR 24.99 dB) results in strong noise reduction while maintaining structural details effectively. DCT performs better, with a noise variance ranging from 10 to 40, achieving 31.82 dB to 20.19 dB to preserve low frequency components. PCA achieves moderate noise reduction at  $\sigma = 10$ , with a PSNR of 30.84 dB,

**Figure 5.** Graphical representation of SNR values of various denoising methods at Noise variance ( $\sigma = 10, 20, 30$  and  $40$ ).**Figure 6.** Denoised outcomes of various denoising methods (a) DCT result, (b) PCA result, (c) MSVD result, (d) DWT result.**Figure 7.** Graphical representation of SSIM values of various denoising methods at Noise variance ( $\sigma = 10, 20, 30$  and  $40$ ).

reducing PSNR value as the noise increases, where as MSVD achieved less denoising performance compared to other denoising methods. Overall, the DWT method achieves high PSNR value compared to other existing methods. Table 2 depicts quantitative analysis of SNR, where a higher SNR indicates better noise suppression, resulting in better quality. Among all these methods, DWT achieves the highest SNR value at noise level  $\sigma = 10$  (28.50 dB), providing better noise reduction and edge preservation. Table 3 shows a comparative analysis of SSIM metric using various denoising methods, SSIM method shows superior perceptual results, it is ranging from 0 to 1. A value of 1 indicates the denoised output is similar to clean image.

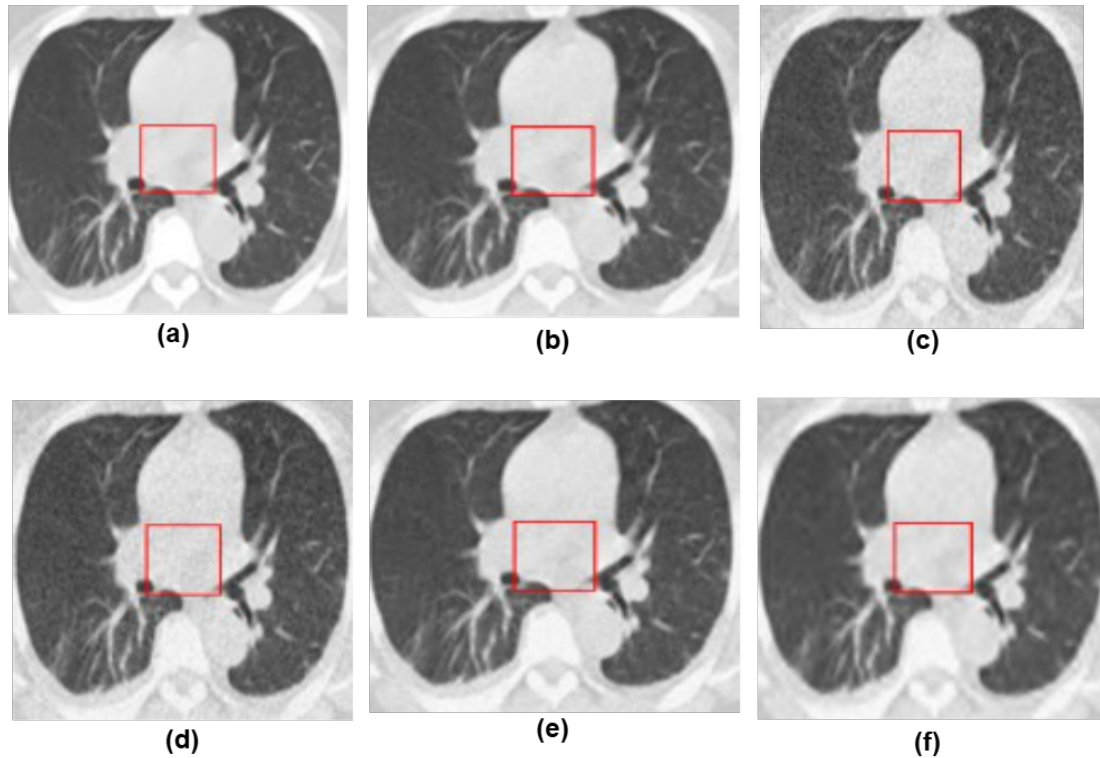


**Figure 8.** LDCT images with rectangular Region of interest (ROI) marked for Zooming analysis (a) Clean CT1 image, (b) Gaussian Noisy CT1 image (Noise variance  $\sigma = 10$ ), (c) DCT method, (d) PCA method, (e) MSVD method, (f) DWT method.

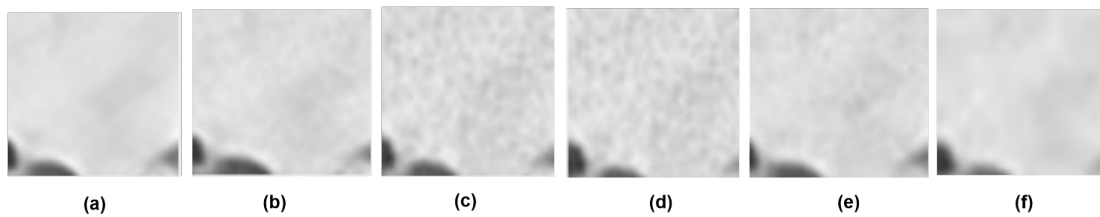


**Figure 9.** Zooming Comparison of ROI using various denoising methods (a) Clean CT1 image, (b) Gaussian Noisy CT1 image (Noise variance  $\sigma = 10$ ), (c) DCT method, (d) PCA method, (e) MSVD method, (f) DWT method.

The SSIM value of DWT method at  $\sigma=10$ , 0.7194, and DCT method shows moderate structural preservation in LDCT images. The PCA and MSVD shows lower SSIM values, indicating less structural preservation. Overall, DWT method shows better noise suppression in terms of PSNR, SNR and SSIM, resulting in better structure retention in LDCT images.

The graphical notation of PSNR, SNR, and SSIM metric values as shown in Figures 4, 5 and 6. The visual quality of denoised outcomes is depicted in Figure 7. The PCA method depicts moderate denoising performance, but face difficulty in preserving finer-textures at higher noise levels. The MSVD denoised images result in over-smoothing, and loss of fine structural details. DCT method performs better noise suppression, drops at higher noise levels but shows better structural preservation at lower

noise intensities. Overall, DWT method provides better visual quality and clarity compared to all other methods. The zooming analysis of different transform domain denoising techniques such as PCA, MSVD, DCT, and DWT, is shown in Figures 8 and 9. Among these methods, the DWT demonstrates superior denoising performance in maintaining edge features and structural clarity compared to zooming analysis. The DCT method preserved image textures moderately, but often introduced blocking artifacts at higher zooming levels. MSVD and PCA methods demonstrated noticeable blurring and loss of fine details, thereby restricting their efficiency for fine structural visualization. Overall, the DWT method was confirmed to be a valid approach for examining zoomed CT images, providing the best trade-off between noise suppression and detail preservation.

In addition to CT image denoising efficiency, computational efficiency was analyzed. The computational cost of transform-based denoising techniques plays a major role in assessing their applicability for healthcare-related and real-time CT-imaging applications. From the perspective of computational cost, the DWT method demonstrates higher efficiency because of its linear time complexity  $O(N)$  for each decomposition level, making it suitable for large scale image datasets. The PCA method involves computing the image's covariance matrix after eigen-value decomposition, which is accompanied by cubic complexity of  $O(N^3)$ , where  $N$  represents the dimensionality (number of features) of the data. This step becomes a limitation for higher resolution CT images. The MSVD denoising method is computationally more challenging than other denoising methods. This method applies singular value decomposition in an iterative way across multiresolution levels. Each SVD process has a computational complexity of nearly  $O(M \times N^2)$  for each image matrix size ( $M \times N$ ) times, and repeated decomposition throughout scales increases runtime drastically. In practice, this method results in longer processing times for 2-Dimensional slice CT image datasets. The DCT method obtains a better computational efficiency due to the use of faster algorithms, such as Fast Fourier transform, and its time complexity is  $O(N \log N)$ , where  $n$  denotes a total number of image pixels. This method provides rapid-transformation, and the inverse transformation is effectively useful for CT image denoising. However, this method may generate blocking artifacts at increased noise intensity levels. Overall, the MSVD denoising method has the lowest computational cost and higher accuracy compared to other standard denoising methods such as PCA, MSVD, and DCT.

## 5 Conclusion

CT scan images are often compromised by Gaussian noise in LDCT images. The DWT-based transform domain denoising method performs better than other standard denoising methods, such as PCA, MSVD, and DCT methods, in CT image noise reduction and fine structural preservation. The quantitative results in terms of PSNR, SNR, and SSIM under varying noise variances. The DWT method has multi-resolutional decomposition extracts local and global features to obtain visually more detailed accurate image reconstructions. Compared to other denoising methods, DWT shows fewer artifacts and fine texture preservation. Therefore, the DWT method

is a robust and visually coherent denoising method among all other techniques.

## 5.1 Limitations

The present research study has identified some limitations. The quantitative and qualitative analysis was carried out using a single dataset that included synthetic noise, which may not fully exhibit the authentic LDCT noisy images and patient-caused artifacts. Transform based denoising techniques, such as MSVD and PCA, are computationally demanding, which can restrict the scalability of high-resolution images in real-time clinical settings. The inclusion of recent state-of-the-art learning-based noise reduction methods would provide a more extensive benchmark to enhance diagnostic accuracy.

## Data Availability Statement

Data will be made available on request.

## Funding

This work was supported without any funding.

## Conflicts of Interest

The authors declare no conflicts of interest.

## Ethical Approval and Consent to Participate

Not applicable. This study is based on a publicly available dataset (SARS-CoV-2 CT-scan dataset) and does not involve any new collection of human or animal data, patient interactions, or ethical interventions requiring approval from an institutional review board.

## References

- [1] Sadia, R. T., Chen, J., & Zhang, J. (2024). CT image denoising methods for image quality improvement and radiation dose reduction. *Journal of applied clinical medical physics*, 25(2), e14270. [[Crossref](#)]
- [2] Abuya, T. K., Rimiru, R. M., & Okeyo, G. O. (2023). An image denoising technique using wavelet-anisotropic gaussian filter-based denoising convolutional neural network for CT images. *Applied sciences*, 13(21), 12069. [[Crossref](#)]
- [3] Kumar, R. R., & Priyadarshi, R. (2025). Denoising and segmentation in medical image analysis: A comprehensive review on machine learning and deep learning approaches. *Multimedia Tools and Applications*, 84(12), 10817-10875. [[Crossref](#)]

- [4] Zhang, F., Liu, J., Liu, Y., & Zhang, X. (2023). Research progress of deep learning in low-dose CT image denoising. *Radiation protection dosimetry*, 199(4), 337-346. [Crossref]
- [5] Mao, J., Sun, L., Chen, J., & Yu, S. (2025). Overview of Research on Digital Image Denoising Methods. *Sensors*, 25(8), 2615. [Crossref]
- [6] Zhou, Y., Kong, Z., Huang, T., Ahn, E., Li, H., & Ding, L. (2024). WaveletDFDS-Net: A Dual Forward Denoising Stream Network for Low-Dose CT Noise Reduction. *Electronics*, 13(10), 1906. [Crossref]
- [7] Esfahani, E. E., & Gouran, A. (2025). Low-dose CT using a nonlocal and nonlinear principal component analysis for image restoration. *IEEE Transactions on Radiation and Plasma Medical Sciences*. [Crossref]
- [8] Hosen, M. A., Moz, S. H., Kabir, S. S., Adnan, M. N., & Galib, S. M. (2024). In-depth exploration of digital image watermarking with discrete cosine transform and discrete wavelet transform. *Indonesian Journal of Electrical Engineering and Computer Science*, 33(1), 581-90. [Crossref]
- [9] Katageri, G. S., & Swamy, P. S. (2025). Denoising and analysis of synthetic aperture radar images using improved weight threshold technique in curvelet transform frequency domain. *Multimedia Tools and Applications*, 84(12), 10173-10194. [Crossref]
- [10] Bhosekar, S., Singh, P., & Garg, D. (2025, January). A Comparative Analysis of Multi-Modal Medical Image Fusion Techniques using MSVD, WPD, PCA, and DWT. In *2025 International Conference on Cognitive Computing in Engineering, Communications, Sciences and Biomedical Health Informatics (IC3ECSBHI)* (pp. 923-927). IEEE. [Crossref]
- [11] Alnuaimy, A. N., Jawad, A. M., Abdulkareem, S. A., Mustafa, F. M., Ivanchenko, S., & Toliupa, S. (2024, April). Bm3d denoising algorithms for medical image. In *2024 35th Conference of Open Innovations Association (FRUCT)* (pp. 135-141). IEEE. [Crossref]
- [12] Choi, K. (2024). Self-supervised learning for CT image denoising and reconstruction: a review. *Biomedical Engineering Letters*, 14(6), 1207-1220. [Crossref]
- [13] Lei, Y., Niu, C., Zhang, J., Wang, G., & Shan, H. (2023). CT image denoising and deblurring with deep learning: current status and perspectives. *IEEE Transactions on Radiation and Plasma Medical Sciences*, 8(2), 153-172. [Crossref]
- [14] Zhang, B., Zhang, Y., Wang, B., He, X., Zhang, F., & Zhang, X. (2024). Denoising swin transformer and perceptual peak signal-to-noise ratio for low-dose CT image denoising. *Measurement*, 227, 114303. [Crossref]
- [15] Yuan, J., Zhou, F., Guo, Z., Li, X., & Yu, H. (2023). HCformer: hybrid CNN-transformer for LDCT image denoising. *Journal of Digital Imaging*, 36(5), 2290-2305. [Crossref]
- [16] Soares, E., Angelov, P., Biaso, S., Froes, M. H., & Abe, D. K. (2020). SARS-CoV-2 CT-scan dataset: A large dataset of real patients CT scans for SARS-CoV-2 identification. *MedRxiv*, 2020-04. [Crossref]
- [17] Zubair, M., Helmi, B., Ullah, F., Al-Tashi, Q., Faheem, M., & Khan, A. A. (2024). Enabling predication of the deep learning algorithms for low-dose CT scan image denoising models: A systematic literature review. *IEEE Access*, 12, 79025-79050. [Crossref]



**Swapna Katta** is currently pursuing her Ph.D. in Computer Science and Artificial Intelligence at SR University, Telangana, India. Her research interests focus on medical image processing, particularly CT image denoising and enhancement techniques. She is exploring advanced transform-domain methods to improve image quality in low-dose computed tomography. (Email: swapnakondam1@gmail.com)



**Deepak Garg** Deepak Garg received his Ph.D. in Computer Science with a specialization in Efficient Algorithm Design. He has over 25 years of academic and research experience. His current research interests include algorithm optimization, computational intelligence, and their applications in medical image processing. He is currently a faculty member at SR University, Telangana, India. (Email: deepak.garg@sru.edu.in)